

Electronic Supplementary Information for Thermodynamics of ion binding and occupancy in potassium channels

Zhifeng Jing,[†] Joshua A. Rackers,[‡] Lawrence R. Pratt,[§] Chengwen Liu,[†] Susan B. Rempe, ^{‡*}
Pengyu Ren^{†*}

*Susan B. Rempe, Pengyu Ren
Email: slrempe@sandia.gov, pren@mail.utexas.edu

This PDF file includes:

Supplementary text
Figures S1 to S6
Tables S1 to S4
SI References

Supplementary Information Text

Materials and Methods

Quantum mechanical (QM) calculations. QM gas-phase binding and interaction energies were calculated to validate the AMOEBA force field. Geometry optimization was carried out with MP2/aug-cc-pVTZ/def2TZVPP by using Gaussian09¹ or Psi4 package.² MP2, DFT and CCSD(T) single-point calculations were performed using Psi4. The QM energies were compared with AMOEBA with several sets of parameters,³⁻⁵ as explained in Fig. S1 caption. Counterpoise correction in Gaussian09 and Psi4 was applied for all interaction energies.

MD simulations. For AMOEBA simulations, the equation of motion was integrated by the RESPA integrator with an outer timestep of 2 fs and the temperature was controlled by the Bussi thermostat at 298 K. The electrostatics was treated by particle-mesh Ewald (PME) method with a real-space cutoff of 8 Å and grid size of 0.9 Å, and the polarization was solved by the OPT4 algorithm. The vdW cutoff was 12 Å. For CHARMM simulations, the leapfrog integrator was used and all hydrogen atoms were constrained by SETTLE or LINCS algorithms to allow for a timestep of 2 fs. The Berendsen/Bussi thermostat for equilibration/production and the Berendsen barostat for equilibration were used to maintain the system temperature and pressure. The cutoffs for real-space electrostatics and vdW were set to 12 Å and long-range electrostatics was treated by PME with grid size of 1.2 Å. The initial equilibration of the DOPC systems employed semi-isotropic barostat. The DOPC systems were equilibrated through the procedure recommended by CHARMM-GUI, which consists of multiple steps with decreasing restraints on protein backbone and sidechain heavy atoms and on the torsional angles of the lipids.

Free energy calculation. The standard protocol as in our previous work⁶⁻⁷ was used to calculate the standard binding free energies. In absolute binding free energy calculations using AMOEBA, a total of 18 alchemical states were set up to connect the two end states. The electrostatic interactions between the ligand (ion or water in our simulations) and the environment were first gradually decoupled in 10 steps ($\lambda = 1.0, 0.9, 0.8, \dots, 0.0$) before the vdW interactions were turned off in 8 steps ($\lambda = 1.0, 0.9, 0.8, 0.7, 0.6, 0.55, 0.5, 0.0$). The default vdW soft-core parameters in Tinker were used. A restraint on the ligand in the decoupled state was applied to avoid bad convergence and an analytical correction was added to account for the free energy change between the standard state (1 mol/L in both gas phase and solution phase) and the constrained state. Flat-bottom restraints between the ligand and the center of mass of the binding sites defined by carbonyl groups were used to maintain the designated ion configurations in the bound state. These flat-bottom restraints have a radius of 1.8 Å and a force constant of 50 kcal/mol/Å², which specify a volume similar to the size of the binding sites. The restraints were gradually changed to a harmonic restraint with force constant 15 kcal/mol/Å in the fully decoupled state ($\lambda = 0.0$). The free energy change from the decoupled state to the standard state in gas phase was analytically calculated to be 6.23 kcal/mol.⁸ For each state, the simulations consist of 1-ns NVT equilibration and 2-ns NVT production. The production simulation was used for free energy perturbation using the Bennet acceptance ratio (BAR) method.

A similar protocol was used for GROMACS CHARMM calculations, with a few differences noted below. A total of 20 alchemical states were set up, with 10 states for electrostatics and 10 states for vdW ($\lambda = 1.0, 0.9, 0.8, 0.7, 0.6, 0.55, 0.5, 0.4, 0.2, 0.0$), due to the different vdW soft-core function. The flat-bottom restraints were kept constant with a radius of 1.8 Å and a force constant of 47.8 kcal/mol/Å² (or 40000 kJ/mol/nm² in GROMACS units and convention), because mutation of the radius was not supported. The analytical standard state correction was 2.49 kcal/mol. The simulations consist of 2-ns NPT equilibration and 4-ns NVT production. VdW softcore parameters were sc-alpha = 0.5, sc-power = 1, sc-r-power = 6, sc-sigma = 0.3. No coulomb softcore was used.

The AMOEBA relative binding free energies were calculated by mutating the force field parameters. 15 steps were used for water-K⁺ relative binding free energy. The O vdW/polarizability parameters were mutated to those of K⁺ in 3 steps, then the O charge was changed to +1 in 10 steps while O dipole/quadruple and H multipole/polarizability were changed to 0. Last, the H vdW was turned off in 2 steps. For Na-K relative binding free energy, all parameters were linearly changed from Na to K in 4 steps. 1-ns equilibration and 2-ns production simulations were conducted for each state.

Using the 4-ion configuration as a reference, the free energy of each 3-ion configuration was derived from one double decoupling calculation. In addition, the free energy of water-K⁺-K⁺-K⁺ was also calculated by water-K⁺ relative binding at S1 using AMOEBA, which gives 0.65 ± 0.16 kcal/mol compared to 0.76 ± 0.21 kcal/mol from K⁺ binding at S1. For AMOEBA, the free energy of water-K⁺-water-K⁺ was calculated by water-K⁺ relative binding at S3. Then water-K⁺-vacancy-K⁺ was calculated by additional water binding at S3. The free energy of water-K⁺-vacancy-K⁺ from this path is 5.06 ± 0.30 kcal/mol, compared to 5.60 ± 0.30 kcal/mol from K⁺ binding at S3. The agreement from different paths further verifies the convergence of the free energy calculation. For CHARMM, water-K⁺-vacancy-K⁺ was first calculated by K⁺ binding at S3, and then water-K⁺-water-K⁺ was calculated by an additional water binding at S3.

For the collapsed conformation of KcsA and the conductive conformation of KcsA-G77A, the 2-ion configurations in the crystal structures were used as a reference.

The AMOEBA absolute binding free energy calculations used the amoebapro13 parameters. The results of mod1 and mo2 parameters were obtained by FEP from amoebapro13 to the modified parameters. Since both are small modifications, three steps were enough to obtain converged free energies.

The total free energy for 1-ion, 2-ion or 3-ion configurations can be calculated by summing up the partition function of each configuration,

$$\Delta G = -RT \ln [\sum_i \exp(-\Delta G_i/RT)]. \quad (S1)$$

When one configuration has much lower free energy than others, the total free energy can be approximated by the free energy of this configuration. The two 2-ion configurations that we calculated are assumed to have the lowest free energies. Using Eq. (S1) and the data from Table S1, the binding free energy for the second, third and fourth ion can be calculated and compared to experiment. For G77A mutant, we were unable to calculate the free energy for the only one ion at S4 since this configuration is very unstable.

Similarly, the Na⁺-K⁺ relative binding free energy can be calculated by integrating possible configurations. For the conductive conformation of KcsA, only Na⁺-K⁺-K⁺-K⁺ and K⁺-K⁺-K⁺-Na⁺ were calculated and they have similar free energy. For the collapsed conformation of KcsA and the conductive conformation of G77A, the relative free energy was calculated as ΔG from 2 Na⁺ configuration to 1 Na⁺/1 K⁺ configurations. The most stable 1 Na⁺/1 K⁺ configuration are Na⁺-vacancy-vacancy-K⁺ and water-Na⁺-water-K⁺, respectively.

The relative enthalpy of each ion configuration was calculated by the average energy from 2 ns NVT simulations of the same system at respective configuration. The same restraints as in the FEP calculation were used to maintain the ion configurations.

PMF calculation. In both 1-D and 2-D PMF calculations, the spacing between windows was 0.35 Å and the force constant was 20 kcal/mol/Å. The initial structures were generated by pulling the ion(s) to the desired position(s) in 200-500 ps simulations, and at least two 200-ps simulations were performed at each window in the production run. The center of mass of the SF backbone atoms were restrained at the starting position. The 1-D PMF of the single vacancy model consists of multiple steps. First the ion at S1 was pulled out of the SF to the extracellular side, then the ion at S2 was pulled to S1, then the ion at S3 was pulled to S2, then the ion at S4 was pulled to S3, and in the last step the ion in the cavity was pulled into S4. For the 2-D PMF of the soft knock-on mechanism, the z-coordinates of the ions at S4 and the cavity were used as the reaction coordinates. The ion at S4 was moved upward to S2, and the z-direction distance between the two ions were scanned between 3.0 and 7.5 Å, which covers most likely intermediate states.

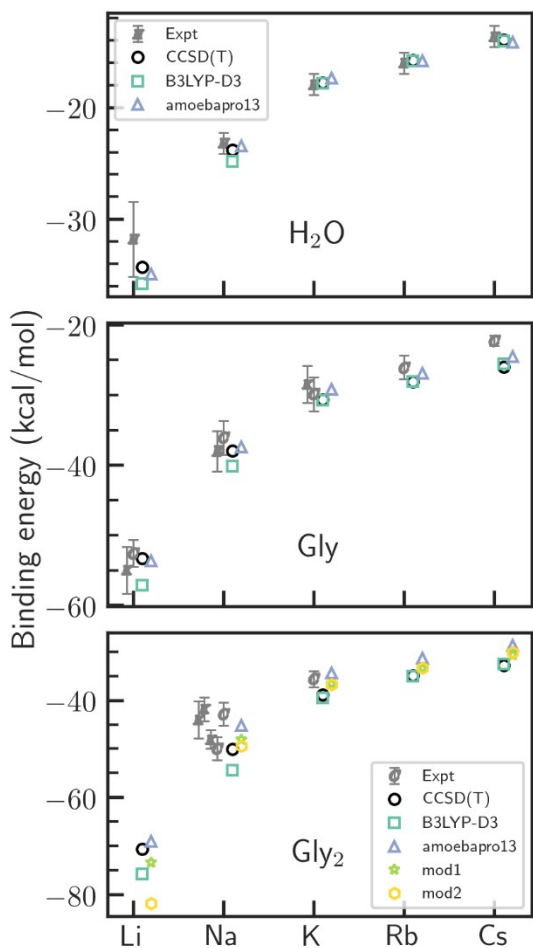


Fig. S1. Comparison of experimental, QM and AMOEBA gas-phase binding energy. The binding energy is evaluated at 0 K. C: threshold collision-induced dissociation; E: single temperature equilibrium; K: kinetic method results.⁹ The geometries and deformation energies are obtained by using MP2/aug-cc-pvtz. CCSD(T) interaction energies are calculated by MP2/CBS + δ CCSD(T)/aug-cc-pvdz. The aug-cc-pvdz basis set was used with B3LYP-D3. The parameter “mod1” is amoebapro13 + modification of C=O dipole based on ion-dipeptide interaction; the parameter “mod2” is amoebapro13 + modification of C=O polarizabilities according to Liu et al.³ The parameter “mod2” is used in simulations reported in the main text.

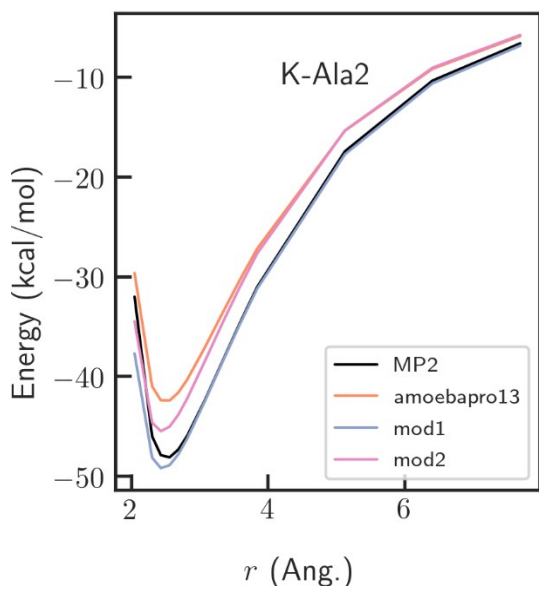


Fig. S2. Comparison of QM and AMOEBA K+-dialanine interaction energy. The parameters “mod1” and “mod2” is defined in the caption of Fig. S1.

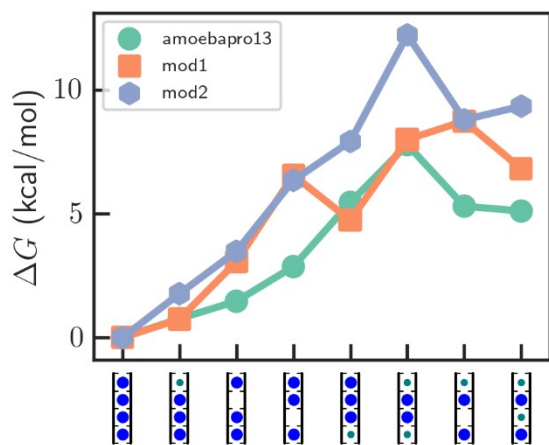


Fig. S3. Relative free energies of K⁺ in KcsA calculated by different parameters.

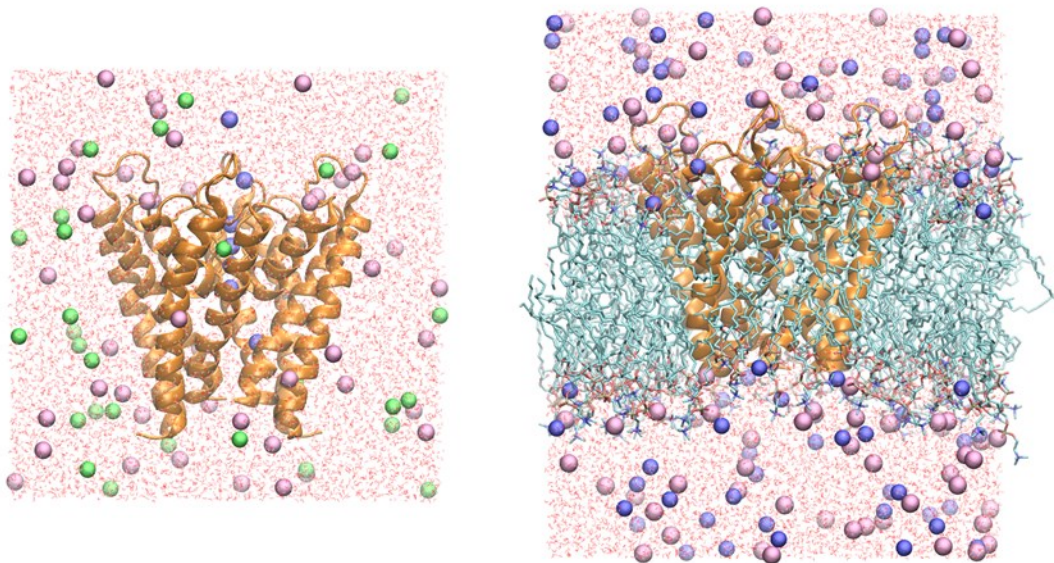
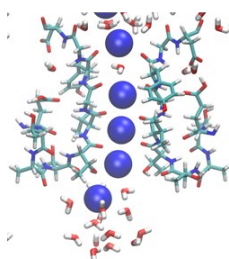
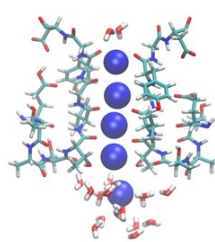


Fig. S4. Model systems for simulations. KcsA in water box (PDB 1k4c) and KcsA in DPOC bilayer (PDB 4fb6). Protein, lipid, ion and water are shown in ribbons, sticks, spheres and lines, respectively. K⁺, Na⁺, Cl⁻ ions are colored in blue, green and purple.

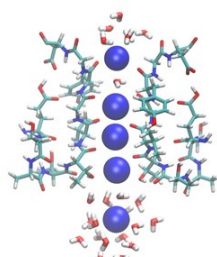
KcsA in DOPC



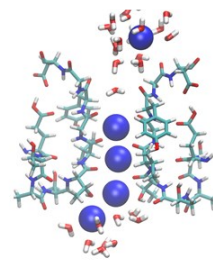
KcsA in water



61%



26%



13%

Fig. S5. Representative structures of MD simulations using AMOEBA simulations of KcsA in DOPC and in water. Two 100-ns simulations were conducted for each system. All simulations started from the four-ion configuration. The simulations in DOPC quickly converge to one major configuration. For the simulations in water, multiple reversible binding/unbinding events were observed. The percentages of major configurations were calculated for the last 80 ns.

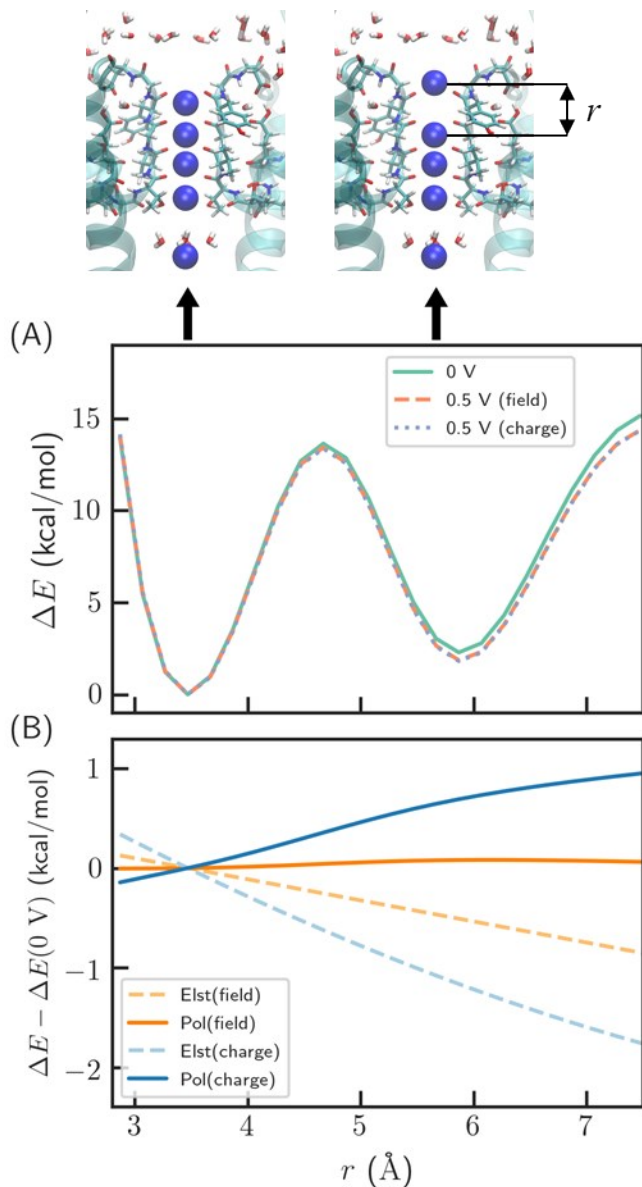


Fig. S6. Effect of membrane potential on the ion interactions in KcsA. (A) Relative energy as a function of ion-ion distance calculated by AMOEBA. “0 V” means no membrane potential, which is identical to the AMOEBA results in **Fig. 2**; “0.5 V (field)” and “0.5 V (charge)” indicate a membrane potential of 0.5 V, represented by an external electric field of 0.0935 V/nm in the z-direction and by two extra K⁺/Cl⁻ ions on each side of the membrane with surface area of 64.3 nm². (B) Change in electrostatic and polarization energy due to the membrane potential. The energy was calculated using the crystal structure (PDB ID: 1k4c) embedded in DOPC bilayer. The two methods for representing the membrane potential have similar total energies, but different energy components. When using the external electric field, the change in polarization energy is negligible.

Table S1. Summary of AMOEBA binding free energy data (kcal/mol).

PDB	Conf. ^a	amoeba13		amoeba13		amoeba13		mod1		mod2	
		→mod1 ^b	sd ^c	→mod2	sd	sd	sd	sd	sd	sd	
1k4c	KKKK	-25.85	0.10	-80.06	0.16	0.00	0.22	0.00	0.24	0.00	0.27
1k4c	wKKK	-25.87	0.12	-79.42	0.17	0.70	0.19	0.68	0.22	1.34	0.25
1k4c	K0KK	-24.25	0.15	-78.41	0.17	1.46	0.21	3.06	0.26	3.12	0.27
1k4c	KK0K	-22.17	0.15	-76.95	0.15	2.86	0.19	6.54	0.24	5.98	0.24
1k4c	KKKw	-26.57	0.23	-77.97	0.17	5.45	0.26	4.73	0.35	7.54	0.31
1k4c	wKKw	-25.64	0.16	-76.01	0.16	7.78	0.50	7.99	0.52	11.84	0.52
1k4c	wK0K	-22.42	0.16	-76.95	0.15	5.36	0.32	8.79	0.36	8.48	0.35
1k4c	wKwK	-24.14	0.48	-76.19	0.16	5.06	0.38	6.77	0.61	8.93	0.41
6nfu	KKwK	-25.46	0.15	-76.73	0.16	10.17	0.11	12.52	0.19	8.97	0.19
6nfu	wKwK	-27.80	0.14	-75.53	0.16	0.00	0.22	0.00	0.26	0.00	0.27
6nfu	wwwK	-26.40	0.25	-73.51	0.17	7.56	0.28	8.96	0.38	9.58	0.33

^a In the “Conf.” column, the four-letter code indicates the species at the four binding site. “K”, “w” and “0” indicates K⁺, water and vacancy, respectively. For example, “wK0K” means water-K⁺-vacancy-K⁺. Also, vacancy at the 1st or 4th position means water-bound and is only for convenience, since no restraints were applied to prevent water from occupying S1 and S4.

^b “amoeba13 → mod1” means the relative free energy for changing the force field parameter from amoeba13 to mod1, and similarly for “amoeba13 → mod2”.

^c “sd” means one standard deviation for the value in the preceding column.

Table S2. AMOEBA binding free energy data (kcal/mol).^a

PDB	A	B	C	A→C				B→C
				dG_raw	dG_std	dG	sd(dG)	dG
1k4c	K(g)	K(aq)	K(aq)	-75.80	0.00	-75.80	0.22	0.00
1k4c	0KKK + K(g)	0KKK + K(aq)	KKKK	-82.79	6.23	-76.56	0.21	-0.76
1k4c	K0KK + K(g)	K0KK + K(aq)	KKKK	-83.49	6.23	-77.26	0.21	-1.46
1k4c	KK0K + K(g)	KK0K + K(aq)	KKKK	-84.89	6.23	-78.66	0.19	-2.86
1k4c	KKK0 + K(g)	KKK0 + K(aq)	KKKK	-87.48	6.23	-81.25	0.26	-5.45
1k4c	0K0K + K(g)	0K0K + K(aq)	0KKK	-86.93	6.23	-80.70	0.20	-4.90
1k4c	0KK0 + K(g)	0KK0 + K(aq)	0KKK	-89.05	6.23	-82.82	0.45	-7.02
6nfu	w0wK + K(g)	w0wK + K(aq)	wKwK	-89.59	6.23	-83.36	0.28	-7.56
6nfu	w(aq)	K(aq)	K(aq)	-69.97	-2.36	-72.33	0.13	0.00
1k4c	wKKK+w(aq)	wKKK+K(aq)	KKKK+w(aq)	-72.98	0.00	-72.98	0.16	-0.65
1k4c	wKwK+w(aq)	wKwK+K(aq)	wKKK+w(aq)	-76.49	0.00	-76.49	0.16	-4.17
6nfu	wKwK+w(aq)	wKwK+K(aq)	KKwK+w(aq)	-62.15	0.00	-62.15	0.11	10.17
water	w(g)	w(aq)	w(aq)	-6.10	2.36	-3.74	0.10	0.00
1k4c	wK0K + w(g)	wK0K + w(aq)	wKwK	-10.16	6.23	-3.93	0.20	-0.19
1k4d	000K + K(g)	000K + K(aq)	K00K	-94.63	6.23	-88.40	0.26	-12.60
1k4d	K000 + K(g)	K000 + K(aq)	K00K	-86.93	6.23	-80.70	0.52	-4.90
6nfu	wKw0 + K(g)	wKw0 + K(aq)	wKwK	-88.02	6.23	-81.79	0.22	-5.99
water	K(aq)	Na(aq)	Na(aq)	-17.3	0.00	-17.30	0.08	0.00
1k4c	KKKK + K(aq)	KKKK + Na(aq)	NaKKK + K(aq)	-14.96	0.00	-14.96	0.18	2.34
1k4c	KKKK + K(aq)	KKKK + Na(aq)	KKKNa + K(aq)	-15.5	0.00	-15.50	0.09	1.80
1k4d	K00K + K(aq)	K00K + Na(aq)	Na00K + K(aq)	-23.51	0.00	-23.51	0.23	-6.21
1k4d	K00K + K(aq)	K00K + Na(aq)	K00Na + K(aq)	-16.18	0.00	-16.18	0.19	1.12
1k4d	K00K + 2 K(aq)	K00K + 2 Na(aq)	Na00Na + 2 K(aq)	-39.17	0.00	-39.17	0.34	-4.57
6nfu	wKwK + K(aq)	wKwK + Na(aq)	wNawK + K(aq)	-20.39	0.00	-20.39	0.25	-3.09
6nfu	wKwK + K(aq)	wKwK + Na(aq)	wKwNa + K(aq)	-13.04	0.00	-13.04	0.18	4.26
6nfu	wKwK + 2 K(aq)	wKwK + 2 Na(aq)	wNawNa + 2 K(aq)	-34.35	0.00	-34.35	0.35	0.25

^a Results of each binding free energy calculation. A, B and C are three thermodynamic states. Same as in Table S1, the codes denotes the configuration in the SF. “K”, “Na”, “w” and “0” denote K⁺, Na⁺, water and vacancy, respectively. Vacancy at the 1st or 4th position means water-bound and is only for convenience, since no restraints were applied to prevent water from occupying S1 and S4. “(g)” and “(aq)” means gas phase and aqueous phase, respectively. Our FEP simulations produce results for A→C reactions. The free energy for reaction B→C is calculated from the difference of two A→C reactions. The standard state is 55.5 mol/L for water in aqueous phase and 1 mol/L otherwise. “dG_raw” is the raw results from FEP, “dG_std” is the free energy between simulated state (e.g. restrained ligand in gas phase) and the standard state.

Table S3. Summary of CHARMM binding free energy at different conditions (kcal/mol).^a

Conf.	C36m	C36m/dopc	C36m/200K	C36m-ECC	C36m-ECC/dopc
KKKK	0.00	0.00	0.00	0.00	0.00
0KKK	-5.37	-9.62	-5.19	3.66	2.03
K0KK	-10.21	-18.52	-10.76	4.38	2.80
KK0K	-11.38	-21.03	-13.28	3.80	0.66
KKK0	-5.25	-20.66	-4.30	5.41	3.18
wK0K	-2.85	-14.01		12.10	8.15
wKKw	-6.69	-17.52		12.02	9.81
wKwK	-2.60	-13.14		8.35	4.14

^a Unless otherwise noted, the results are from solvated protein at 298 K. "dopc" indicates simulations of protein embedded in DOPC bilayer. "200K" indicates simulations at 200 K.

Table S4. CHARMM binding free energy data (kcal/mol). The electronic part of the ECC solvation free energy is omitted.

ff	T (K)	Box	A	B	C	A→C				B→C
						dG_raw	dG_std	dG	sd(dG)	dG
C36m	298	1k4c/water	K(g)	K(aq)	K(aq)	-71.89	0.00	-71.89	0.13	0.00
C36m	298	1k4c/water	0KKK + K(g)	0KKK + K(aq)	KKKK	-69.01	2.49	-66.52	0.22	5.37
C36m	298	1k4c/water	K0KK + K(g)	K0KK + K(aq)	KKKK	-64.17	2.49	-61.68	0.08	10.21
C36m	298	1k4c/water	KK0K + K(g)	KK0K + K(aq)	KKKK	-63.00	2.49	-60.51	0.11	11.38
C36m	298	1k4c/water	KKK0 + K(g)	KKK0 + K(aq)	KKKK	-69.13	2.49	-66.64	0.31	5.25
C36m	298	1k4c/water	0K0K + K(g)	0K0K + K(aq)	0KKK	-76.91	2.49	-74.42	0.51	-2.53
C36m	298	1k4c/water	0KK0 + K(g)	0KK0 + K(aq)	0KKK	-73.07	2.49	-70.58	0.44	1.31
C36m	298	1k4c/water	w(g)	w(aq)	w(aq)	-6.41	2.36	-4.05	0.01	0.00
C36m	298	1k4c/water	wK0K + w(g)	wK0K + w(aq)	wKwK	-6.30	2.49	-3.81	0.06	0.24
C36m	298	1k4c/dopc	K(g)	K(aq)	K(aq)	-74.84	0.00	-74.84	0.22	0.00
C36m	298	1k4c/dopc	0KKK + K(g)	0KKK + K(aq)	KKKK	-67.71	2.49	-65.22	0.20	9.62
C36m	298	1k4c/dopc	K0KK + K(g)	K0KK + K(aq)	KKKK	-58.81	2.49	-56.32	0.12	18.52
C36m	298	1k4c/dopc	KK0K + K(g)	KK0K + K(aq)	KKKK	-56.30	2.49	-53.81	0.13	21.03
C36m	298	1k4c/dopc	KKK0 + K(g)	KKK0 + K(aq)	KKKK	-56.67	2.49	-54.18	0.36	20.66
C36m	298	1k4c/dopc	0K0K + K(g)	0K0K + K(aq)	0KKK	-72.95	2.49	-70.46	0.18	4.38
C36m	298	1k4c/dopc	0KK0 + K(g)	0KK0 + K(aq)	0KKK	-69.43	2.49	-66.94	0.09	7.90
C36m	298	1k4c/dopc	w(g)	w(aq)	w(aq)	-6.74	2.36	-4.38	0.08	0.00
C36m	298	1k4c/dopc	wK0K + w(g)	wK0K + w(aq)	wKwK	-6.00	2.49	-3.51	0.08	0.87
C36m	200	1k4c/water	K(g)	K(aq)	K(aq)	-74.17	0.00	-74.17	0.05	0.00
C36m	200	1k4c/water	0KKK + K(g)	0KKK + K(aq)	KKKK	-71.47	2.49	-68.98	0.08	5.19
C36m	200	1k4c/water	K0KK + K(g)	K0KK + K(aq)	KKKK	-65.91	2.49	-63.42	0.61	10.76
C36m	200	1k4c/water	KK0K + K(g)	KK0K + K(aq)	KKKK	-63.38	2.49	-60.89	0.26	13.28
C36m	200	1k4c/water	KKK0 + K(g)	KKK0 + K(aq)	KKKK	-72.36	2.49	-69.87	0.52	4.30
C36m-ECC	298	1k4c/water	K(g)	K(aq)	K(aq)	-31.10	0.00	-31.10	0.06	0.00
C36m-ECC	298	1k4c/water	0KKK + K(g)	0KKK + K(aq)	KKKK	-37.25	2.49	-34.76	0.57	-3.66
C36m-ECC	298	1k4c/water	K0KK + K(g)	K0KK + K(aq)	KKKK	-37.97	2.49	-35.48	0.26	-4.38
C36m-ECC	298	1k4c/water	KK0K + K(g)	KK0K + K(aq)	KKKK	-37.39	2.49	-34.90	0.18	-3.80
C36m-ECC	298	1k4c/water	KKK0 + K(g)	KKK0 + K(aq)	KKKK	-39.00	2.49	-36.51	1.16	-5.41
C36m-ECC	298	1k4c/water	0K0K + K(g)	0K0K + K(aq)	0KKK	-42.02	2.49	-39.53	0.79	-8.44
C36m-ECC	298	1k4c/water	0KK0 + K(g)	0KK0 + K(aq)	0KKK	-41.95	2.49	-39.46	1.25	-8.36
C36m-ECC	298	1k4c/water	w(g)	w(aq)	w(aq)	-6.12	2.36	-3.76	0.07	0.00
C36m-ECC	298	1k4c/water	wK0K + w(g)	wK0K + w(aq)	wKwK	-10.00	2.49	-7.51	0.13	-3.75
C36m-ECC	298	1k4c/dopc	K(g)	K(aq)	K(aq)	-33.39	0.00	-33.39	0.05	0.00
C36m-ECC	298	1k4c/dopc	0KKK + K(g)	0KKK + K(aq)	KKKK	-37.91	2.49	-35.42	0.20	-2.03
C36m-ECC	298	1k4c/dopc	K0KK + K(g)	K0KK + K(aq)	KKKK	-38.68	2.49	-36.19	0.26	-2.80

C36m-ECC	298	1k4c/dopc	KK0K + K(g)	KK0K + K(aq)	KKKK	-36.54	2.49	-34.05	0.36	-0.66
C36m-ECC	298	1k4c/dopc	KKK0 + K(g)	KKK0 + K(aq)	KKKK	-39.07	2.49	-36.58	0.06	-3.18
C36m-ECC	298	1k4c/dopc	0K0K + K(g)	0K0K + K(aq)	0KKK	-42.01	2.49	-39.52	0.61	-6.13
C36m-ECC	298	1k4c/dopc	0KK0 + K(g)	0KK0 + K(aq)	0KKK	-43.66	2.49	-41.17	0.30	-7.78
C36m-ECC	298	1k4c/dopc	w(g)	w(aq)	w(aq)	-6.59	2.36	-4.23	0.08	0.00
C36m-ECC	298	1k4c/dopc	wK0K + w(g)	wK0K + w(aq)	wKwK	-10.74	2.49	-8.25	0.15	-4.02

SI References

1. Frisch, M. T., G.; Schlegel, H. B.; Scuseria, G.; Robb, M.; Cheeseman, J.; Scalmani, G.; Barone, V.; Mennucci, B.; Petersson, G. Inc, Wallingford, CT 2009, 200., Gaussian 09.
2. Smith, D. G. A.; Burns, L. A.; Simmonett, A. C.; Parrish, R. M.; Schieber, M. C.; Galvelis, R.; Kraus, P.; Kruse, H.; Di Remigio, R.; Alenaizan, A.; James, A. M.; Lehtola, S.; Misiewicz, J. P.; Scheurer, M.; Shaw, R. A.; Schriber, J. B.; Xie, Y.; Glick, Z. L.; Sirianni, D. A.; O'Brien, J. S.; Waldrop, J. M.; Kumar, A.; Hohenstein, E. G.; Pritchard, B. P.; Brooks, B. R.; Schaefer, H. F.; Sokolov, A. Y.; Patkowski, K.; DePrince, A. E.; Bozkaya, U.; King, R. A.; Evangelista, F. A.; Turney, J. M.; Crawford, T. D.; Sherrill, C. D., PSI4 1.4: Open-source software for high-throughput quantum chemistry. *The Journal of Chemical Physics* **2020**, *152* (18), 184108.
3. Liu, C.; Qi, R.; Wang, Q.; Piquemal, J. P.; Ren, P., Capturing Many-Body Interactions with Classical Dipole Induction Models. *J. Chem. Theory Comput.* **2017**, *13* (6), 2751-2761.
4. Shi, Y.; Xia, Z.; Zhang, J.; Best, R.; Wu, C.; Ponder, J. W.; Ren, P., Polarizable Atomic Multipole-Based AMOEBA Force Field for Proteins. *J. Chem. Theory Comput.* **2013**, *9* (9), 4046-4063.
5. Wang, Z. Polarizable Force Field Development, and Applications to Conformational Sampling and Free Energy Calculation. Washington University in St. Louis, St. Louis, Missouri, 2018.
6. Bell, D. R.; Qi, R.; Jing, Z.; Xiang, J. Y.; Mejias, C.; Schnieders, M. J.; Ponder, J. W.; Ren, P., Calculating binding free energies of host-guest systems using the AMOEBA polarizable force field. *Phys. Chem. Chem. Phys.* **2016**, *18* (44), 30261-30269.
7. Qi, R.; Jing, Z.; Liu, C.; Piquemal, J.-P.; Dalby, K. N.; Ren, P., Elucidating the Phosphate Binding Mode of Phosphate-Binding Protein: The Critical Effect of Buffer Solution. *Journal of Physical Chemistry B* **2018**, *122* (24), 6371-6376.

8. Hamelberg, D.; McCammon, J. A., Standard Free Energy of Releasing a Localized Water Molecule from the Binding Pockets of Proteins: Double-Decoupling Method. *J. Am. Chem. Soc.* **2004**, *126* (24), 7683-7689.
9. Rodgers, M. T.; Armentrout, P. B., Cationic Noncovalent Interactions: Energetics and Periodic Trends. *Chem. Rev.* **2016**, *116* (9), 5642-5687.